eNeuro

Research Article: New Research

Integrative Systems

Prenatal Androgen Treatment Does Not Alter the Firing Activity of Hypothalamic Arcuate Kisspeptin Neurons in Female Mice

Amanda G. Gibson,[2] Jennifer Jaime,[2] Laura L. Burger,[1] and Suzanne M. Moenter[1,3,4,5]

https://doi.org/10.1523/ENEURO.0306-21.2021

[1]Departments of Molecular and Integrative Physiology, University of Michigan, Ann Arbor, MI 48109, [2]Neuroscience Graduate Program, University of Michigan, Ann Arbor, MI 48109, [3]Internal Medicine, University of Michigan, Ann Arbor, MI 48109, [4]Obstetrics and Gynecology, University of Michigan, Ann Arbor, MI 48109, and [5]The Reproductive Sciences Program, University of Michigan, Ann Arbor, MI 48109

Abstract

Neuroendocrine control of reproduction is disrupted in many individuals with polycystic ovary syndrome (PCOS), who present with increased luteinizing hormone (LH), and presumably gonadotropin-releasing hormone (GnRH), release frequency, and high androgen levels. Prenatal androgenization (PNA) recapitulates these phenotypes in primates and rodents. Female offspring of mice injected with dihydrotestosterone (DHT) on gestational days 16–18 exhibit disrupted estrous cyclicity, increased LH and testosterone, and increased GnRH neuron firing rate as adults. PNA also alters the developmental trajectory of GnRH neuron firing rates, markedly blunting the prepubertal peak in firing that occurs in three-week (3wk)-old controls. GnRH neurons do not express detectable androgen receptors and are thus probably not the direct target of DHT. Rather, PNA likely alters GnRH neuronal activity by modulating upstream neurons, such as hypothalamic arcuate neurons co-expressing kisspeptin, neurokinin B (gene Tac2), and dynorphin, also known as KNDy neurons. We hypothesized PNA treatment changes firing rates of KNDy neurons in a similar age-dependent manner as GnRH neurons. We conducted targeted extracellular recordings (0.5–2 h) of Tac2-identified KNDy neurons from control and PNA mice at 3wks of age and in adulthood. About half of neurons were quiescent ($<$0.005 Hz). Long-term firing rates of active cells varied, suggestive of episodic activity, but were not different among groups. Short-term burst firing was also similar. We thus reject the hypothesis that PNA alters the firing rate of KNDy neurons. This does not preclude altered neurosecretory output of KNDy neurons, involvement of other neuronal populations, or *in vivo* networks as critical drivers of altered GnRH firing rates in PNA mice.

Key words: arcuate; development; kisspeptin; reproduction

Significance Statement

Prenatal androgenization (PNA) recapitulates key aspects of the common reproductive disorder polycystic ovary syndrome (PCOS). It is postulated that disruptions in the episodic pattern of gonadotropin-releasing hormone (GnRH) secretion in part underly this disorder, yet GnRH neurons do not express androgen receptor to respond directly to elevated androgens. A population of kisspeptin, neurokinin B, and dynorphin-expressing (KNDy) neurons in the hypothalamic arcuate nucleus (ARC) are thought to regulate pulsatile GnRH release and some express androgen receptor. We did not find evidence, however, that PNA altered spontaneous activity of KNDy neurons before puberty at three weeks (3wks) of age or in adulthood. This suggests that PNA likely acts via other components of the broader hypothalamic network to change the patterns of GnRH release.

Received July 18, 2021; accepted September 7, 2021; First published September 9, 2021.
The authors declare no competing financial interests.

Author contributions: A.G.G. and S.M.M. designed research; A.G.G., J.J., L.L.B., and S.M.M. performed research; A.G.G., J.J., L.L.B., and S.M.M. analyzed data; A.G.G. and S.M.M. wrote the paper.

Introduction

Gonadotropin-releasing hormone (GnRH) regulates the secretion of the gonadotropins luteinizing hormone (LH) and follicle-stimulating hormone (FSH) from the anterior pituitary. GnRH is released in an episodic manner that varies in frequency through the female reproductive cycle (Levine and Ramirez, 1982; Moenter et al., 1991). Lower frequency favors synthesis and release of FSH over LH and is important for recruiting ovarian follicles and their subsequent maturation, whereas higher pulse frequency in the mid-late follicular phase favors LH, which drives androgen synthesis (Wildt et al., 1981; Haisenleder et al., 1991). Failure to vary the frequency of GnRH release is thought to be a key neuroendocrine phenotype of the reproductive disorder polycystic ovary syndrome (PCOS).

PCOS is a complex spectrum of reproductive and metabolic phenotypes with postulated genetic and environmental causes. Patients with PCOS often exhibit a persistently high LH (and presumably GnRH) pulse frequency, leading to disrupted follicle maturation and ovulation. Increased LH stimulation also drives hyperandrogenism (McCartney et al., 2002; Dumesic et al., 2015). To investigate the etiology of the disorder, animal models are needed for experimental manipulations and measurements that cannot be conducted in humans. Elevated prenatal androgen (PNA) exposure recapitulates PCOS-like reproductive phenotypes in many species including non-human primates (Dumesic et al., 1997; Abbott et al., 2008, 2017, 2019), sheep (Birch et al., 2003; Veiga-Lopez et al., 2008), and rodents (Sullivan and Moenter, 2004; Foecking et al., 2005). In adult-PNA mice, LH pulse frequency (Moore et al., 2015) and GnRH neuron action potential firing frequency (Roland and Moenter, 2011) are both increased. PNA in mice also alters the developmental trajectory of GnRH neuron firing frequency, which is interesting as aspects of PCOS may emerge around the pubertal transition (McCartney et al., 2002; Rosenfield, 2007). Specifically, in control mice, the firing frequency peaks at 3wks of age before decreasing to adult levels (Dulka and Moenter, 2017). In contrast, the firing frequency in PNA female mice did not vary with age, and it was lower than control mice at 3wks, distinct from the increase observed in PNA adults (Sullivan and Moenter, 2004; Dulka and Moenter, 2017)

The mechanisms by which PNA alters the activity of GnRH neurons are not completely understood. These neurons do not express detectable levels of androgen receptor (Herbison et al., 1996), thus it is likely that upstream neuronal populations are involved in regulating their firing patterns. One such population is in the hypothalamic arcuate nucleus (ARC), specifically neurons that co-express kisspeptin, neurokinin B, and dynorphin (KNDy neurons). KNDy neurons are posited to be involved in the control of pulsatile GnRH, and subsequent LH, secretion (Han et al., 2015; Clarkson et al., 2017; McQuillan et al., 2019). KNDy neurons express receptors for gonadal steroids, including androgen receptor (Smith et al., 2005), and could serve as the site of steroidal feedback that alters GnRH neuron activity and/or a site of action for PNA exposure (Oakley et al., 2009; Caldwell et al., 2017; Vanacker et al., 2017; Walters et al., 2018).

We hypothesized that PNA treatment would alter the firing frequency of KNDy neurons in an age-dependent manner similar to that of GnRH neurons. We tested this by assessing the effect of PNA on the spontaneous firing frequency of KNDy neurons in prepubertal three-week (3wk)-old and adult female mice through long-term extracellular recordings. Specifically, we postulated that PNA treatment would increase KNDy neuron activity relative to controls in adults but reduce activity relative to controls in 3wk-old mice. We also predicted that 3wk-old control mice would exhibit increased KNDy neuron firing frequency relative to control adults and 3wk-old PNA mice.

Materials and Methods

Animals

Mice expressing enhanced green fluorescent protein (GFP) under the control of Tac2 promoter (Tac2-GFP), BAC transgenic mice (015495-UCD/STOCK Tg [Tac2-EGFP]381Gsat, Mouse Mutant Regional Resource Center; http://www.mmrrc.org/) were used to identify KNDy neurons for recording. In mice, *Tac2* encodes neurokinin B, which is co-expressed with kisspeptin and dynorphin in KNDy neurons. Tac2-GFP-identified cells in brain slices used for recording also express kisspeptin and/or dynorphin at high percentages, supporting their identity as KNDy neurons (Ruka et al., 2013). Mice were maintained in a 14/10 h light/dark photoperiod (lights on at 3 A.M. Eastern Standard Time) and had *ad libitum* access to water and either Harlan 2919 chow during pregnancy/lactation or 2916 chow for maintenance. All animal procedures were approved by the University of Michigan Institutional Animal Care and Use Committee.

To generate experimental mice, a Tac2-GFP female and a CD1 female mouse were bred with a C57B/6 male and monitored daily for a copulatory plug (day 1 of pregnancy). The CD1 dam assists in providing maternal care and nutrition. On days 16–18 of pregnancy, dams were injected subcutaneously with 225 μg/d of dihydrotestosterone (DHT) or sesame oil as vehicle. Control offspring from dams for whom timing of pregnancy could not be clearly established were also included in studies without

This work was supported by National Institutes of Health/*Eunice Kennedy Shriver* National Institute of Child Health and Human Development Grants P50HD028934 and R01HD104345. A.G.G. was supported by the National Defense Science and Engineering Graduate Fellowship Program.

Acknowledgements: We thank Elizabeth Wagenmaker for expert technical assistance and Joshua Gibson for computational guidance.

Correspondence should be addressed to Suzanne M. Moenter at smoenter@umich.edu.

https://doi.org/10.1523/ENEURO.0306-21.2021

injections; firing rate from these mice did not differ from vehicle-treated mice (treatment: $F_{(1,22)} = 2.114$, $p = 0.160$; interaction of age and treatment: $F_{(1,22)} = 0.237$, $p = 0.631$). Experiments were conducted on female offspring before weaning at 3wks of age [postnatal day (PND) 18–PND 21] or in adulthood (PND 66–PND 152; median 133). PNA status was confirmed by anogenital distance and estrous cyclicity in adults. Anogenital distance was measured with digital calipers on two to three successive days and averaged for each mouse. Estrous cyclicity was assessed via vaginal cytology and studies on adult females were done on diestrus. Cycle stage was confirmed with uterine mass; one DHT-treated mouse was excluded because of a uterine mass of 136.2 mg, suggestive of incorrect cycle identification based on vaginal cytology.

Brain slice preparation

All solutions were bubbled with 95% O_2/5% CO_2 for at least 15 min before tissue exposure and throughout the procedures. The brain was rapidly removed and cooled for 60 s in ice-cold sucrose saline solution containing the following: 250 mM sucrose, 3.5 mM KCl, 26 mM $NaHCO_3$, 10 mM D-glucose, 1.25 mM Na_2HPO_4, 1.2 mM $MgSO_4$, and 3.8 mM $MgCl_2$. Coronal slices (300 μm) through the hypothalamic region, including the ARC, were cut with a Leica VT1200S (Leica Biosystems). Slices were incubated for 30 min at room temperature in 50% sucrose saline and 50% artificial CSF (ACSF) containing the following: 135 mM NaCl, 3.5 mM KCl, 26 mM $NaHCO_3$, 10 mM D-glucose, 1.25 mM Na_2HPO_4, 1.2 mM $MgSO_4$, and 2.5 mM $CaCl_2$ (pH 7.4). The slices were then held in 100% ACSF at room temperature for between 0.5 and 5.5 h before recording. No differences in results were attributable to duration after brain slice preparation.

Electrophysiological recording

To evaluate the long-term firing patterns of KNDy neurons with minimal disruption of the cell's intrinsic properties, targeted single-unit extracellular recordings were conducted (Nunemaker et al., 2003; Alcami et al., 2012). Individual slices were transferred to a recording chamber mounted on the stage of an Olympus BX51WI upright fluorescent microscope. A constant perfusion of ACSF at a rate of 3 ml/min was established with a MINIPULS 3 peristaltic pump (Gilson). The chamber was maintained at a temperature of 29–32°C with an inline heating system (Warner Instrument Corporation). ACSF was replaced every hour.

Recording electrodes (resistance 2–4 MΩ) were pulled from borosilicate glass (Schott no. 8250; World Precision Instruments) using a Sutter P-97 puller (Sutter Instrument). The pipettes were filled with a HEPES-buffered pipette solution containing the following: 150 mM NaCl, 10 mM HEPES, 10 mM D-glucose, 2.5 mM $CaCl_2$, 1.3 mM $MgCl_2$, and 3.5 mM KCl, pH7.4. At the surface of the brain slice, a small amount of negative pressure was applied to bring the pipette in contact with tissue, facilitating the later formation of a low-resistance seal (<100 MΩ) between the pipette and neuron (Alcami et al., 2012). Recordings were made with one channel of an EPC10 dual patch-clamp amplifier using PatchMaster software (HEKA Elektronic). Cells were held in voltage-clamp with a 0-mV pipette holding potential. Seal resistance was checked every 10–15 min by measuring response to a 5-mV hyperpolarizing step between series. Data were acquired at 10 kHz and filtered at 5 kHz.

Recording duration ranged from 0.5 to 2.6 h (mean ± SEM 71.7 ± 2.9 min; median 60 min). If a cell was not firing at the conclusion of a recording session, either 20 mM-potassium ACSF (two cells) or the neurokinin-3 receptor agonist senktide (100 nM; Phoenix Pharmaceuticals, 42 cells) was bath-applied. If a cell failed to exhibit action currents following either stimulus, recording integrity could not be verified and data analysis was truncated to the last action current, or not included in analyses if there were no spontaneous events. Response to senktide was quantified by comparing the spontaneous firing frequency for the 5 min before addition of senktide to the ACSF to the firing frequency for 5 min, beginning 2 min after senktide reached the bath to allow time for the drug to equilibrate in the chamber and penetrate the slice. This 2-min delay was chosen based on the onset of and peak senktide response across cells.

Analysis

Event detection was completed using IgorPro8 (WaveMetrics) using custom routines, and all events were manually confirmed. The average spontaneous firing rate was calculated for each cell as total events/recording duration. The short-term patterns of neuronal activity were also assessed with custom IgorPro8 routines. Repetitive, grouped firing events are referred to as "bursts" for analysis. To be considered part of a burst, a firing event must occur within a defined "burst window" after the previous event. The burst window for analysis of these KNDy neurons was identified by varying the burst window from 0.01 to 1 s in 10-ms intervals and selecting the burst window that captures the maximal burst frequency for the control cells; this was 230 ms as in prior reports (Vanacker et al., 2017). At the selected burst window, the software characterizes each event as belonging to a burst or as a single spike, then calculates the following parameters: burst frequency, burst duration, intraburst interval, spikes per burst, single spike frequency, and interevent interval. Burst duration and spikes per burst are the averages for all bursts from a given cell. Intraburst interval is the average of intervals between spikes in a burst, whereas interevent interval is the average of intervals greater than the burst window and can occur between bursts, between single spikes or between single spikes and bursts. Short breaks in the recording (typically <2 s) occur at 10- to 15-min intervals to monitor the seal resistance. Intervals that crossed these gaps were not included when calculating cells' averages. Spikes that occurred within 230 ms (i.e., the burst window) of these gaps, or the start or end of the recording, were characterized according to the available information; this could lead to an underestimate of the burst frequency, burst duration, and/or spikes per burst.

PCR to assess arcuate gene expression

Hypothalamic tissue punches were collected to assess the effect of PNA on gene expression. Separate cohorts

Table 1: Probes and primers sequences for PCR experiments (Fig. 5)

Transcript	Probe 5′—>3′	Forward 5′—>3′	Reverse 5′—>3′
Actb	CTG GCC TCA CTG TCC ACC TTC C	GAT TAC TGC TCT GGC TCC TAG	GAC TCA TCG TAC TCC TGC TTG
Syn1	ACG TGT CTA CCC ACA ACT TGT ACC TG	CTT GAG CAG ATT GCC ATG TC	ACC TCA ATA ATG TGA TCC CTT CC
Kiss1	CGG ACT GCT GGC CTG TGG AT	CTG CTT CTC CTC TGT GTC G	TTC CCA GGC ATT AAC GAG TTC
Kiss1r	TCA ATC CGC TGC TCT ATG CCT TCC	CTC ACT GCA TGT CCT ACA GC	GCC TGT CTG AAG TGT GAA CC
Tac2	AGC TTT GTC CTT CAG GCA CCA TGA	CTG CAC TCT TGT CTC TGT CT	ACA GCC GCA AAC AGC AT
Tacr3	TCT CTT GAA GCC TGC ACG AAA TCT TTT G	AGC TCA ACC ATG TAC AAC CC	CTC ATC GTA GCT GGA GAC TTG
Pdyn	TCA ACC CCC TGA TTT GCT CCC TG	GTG CAG TGA GGA TTC AGG ATG	CAT GTC TCC CAC TCC TCT GA
Opkr1	AGA GAA TTG CCC ACT AAG CCC ACC	CAT CAC CGC TGT CTA CTC TG	GGT CTT CAT CTT CGT GTA TCG G
Ar	ACC ACA TGC ACA AGC TGC CTC T	CTG CCT TGT TAT CTA GCC TCA	ATA CTG AAT GAC CGC CAT CTG
Esr1	TGC CTT CCA CAC ATT TAC CTT GAT TCC T	CCT GTT TGC TCC TAA CTT GCT	GAA CCG ACT TGA CGT AGC C
Pgr	AGA TTC AGA AGC CAG CCA GAG CC	CGC CAT ACC TTA ACT ACC TGA G	CCA TAG TGA CAG CCA GAT GC

of mice from those used for recordings were used to collect tissue micro-punches from the ARC. A coronal slice was obtained with an adult mouse brain matrix (1 mm, Zivic Instruments); an initial cut was made just caudal to the optic chiasm, followed by a cut just rostral to the brain stem (2–3 mm thick) for the ARC. Tissue punches were made with a 1.2-mm Palkovits punch. Tissue was immediately homogenized in RLT buffer (QIAGEN) containing 2-mercaptoethanol (1%v/v, Sigma), snap frozen, and stored at −80°C. RNA from was extracted with the RNeasy Micro kit with on-column DNasing (QIAGEN); 240-ng RNA per sample was reverse transcribed with Superscript IV VILO Master Mix (Fisher/Invitrogen). A standard curve of hypothalamic RNA (600, 120, 24, 4.8, and 0 ng/20 μl) was also reverse transcribed (Ruka et al., 2013). The transcripts for: *Kiss1*, *Kiss1r*, *Pdyn*, *Oprk1*, *Tac2*, *Tacr3*, *Ar*, *Esr1*, and *Pgr* were assayed via Taqman quantitative PCR in duplicate with 10-ng cDNA. Data were analyzed by the ΔΔCT method (Bustin, 2002), normalized to *Actb* and *Syn1* and reported relative to 3wk-CON. Primers and Taqman probes were purchased from Integrated DNA Technologies and are reported in Table 1.

Statistics

Data visualization and analyses were conducted with R (R Core Team, 2019) and RStudio (RStudio Team, 2019) using a combination of open-sourced packages (Chang, 2014; Xie, 2014, 2015, 2020; Fox and Weisberg, 2019; Wickham et al., 2019, 2020; Chang et al., 2020; Gohel, 2020a,b; Henry and Wickham, 2020a,b; Kassambara, 2020, 2021; Schauberger and Walker, 2020; Schloerke et al., 2020; Wickham and Hester, 2020; Wickham and Seidel, 2020; Wilke, 2020; Zhu, 2020; Xie et al., 2021) and custom procedures. Additional statistical analyses were conducted with Prism 9 (GraphPad). Data are reported as mean ± SEM, with median illustrated where indicated. For recordings, n is number of cells; for PNA phenotype confirmation and mRNA quantification, n is number of mice. Normality of the data distribution was evaluated with Shapiro–Wilk. Two-way ANOVA (Type III) was conducted to evaluate the main effects and interactions of age and prenatal treatment. Bonferroni correction for multiple comparisons was used as this test is sufficiently robust for non-normally distributed data (Underwood, 1997). The level accepted as significant was set to $p < 0.05$. Statistical tables for two-way ANOVAs report the differences in means and associated 95% confidence interval (CI) defined for age (adult – 3wk), treatment (PNA – control), and interaction ([adult-PNA – adult-CON] – [3wk-PNA – 3wk-CON]).

Software accessibility

The event detection and burst analysis code described in the paper is freely available online at https://gitlab.com/um-mip/coding-project. The R analysis code is freely available online at https://github.com/gibson-amandag/PNA_KNDy. The code for IgorPro and R analysis are also provided as Extended Data 1. Analyses were conducted on a MacBook Pro, Early 2015 version, running macOS Catalina 10.15.7 and on a Mac Mini, 2018 version, running macOS Mojave 10.14.6

Results

PNA characterization

To verify the effects of PNA (225 μg/d of DHT administered to dams on gestational days 16–18), anogenital distance, body mass, and estrous cycles were recorded from adult offspring, including the surviving female littermates of 3wk-old mice that were used for recordings where possible. As adults, PNA mice had a longer anogenital distance (Fig. 1*A*; statistical parameters in Table 2; control $n = 17$ mice from 10 litters, PNA $n = 23$ mice from 11 litters, $p < 0.0001$) and larger body mass (Fig. 1*B*, $p = 0.026$) than control mice. PNA treatment also altered the distribution of days spent in each estrous cycle stage (Fig. 1*C*,*D*, $p < 0.0001$). PNA mice spent more days in diestrus than expected (standardized residual = 7.08) and fewer days in proestrus than expected (standardized residual = −10.11). These results indicate that the PNA treatment was successful.

Spontaneous firing rate

To determine how age and PNA treatment alter the firing activity of KNDy neurons, we conducted targeted, long-term extracellular recordings of Tac2-GFP-identified neurons in the arcuate nucleus of the hypothalamus. Recordings were obtained from both control and PNA mice at either 3wks of age or in adulthood. These neurons

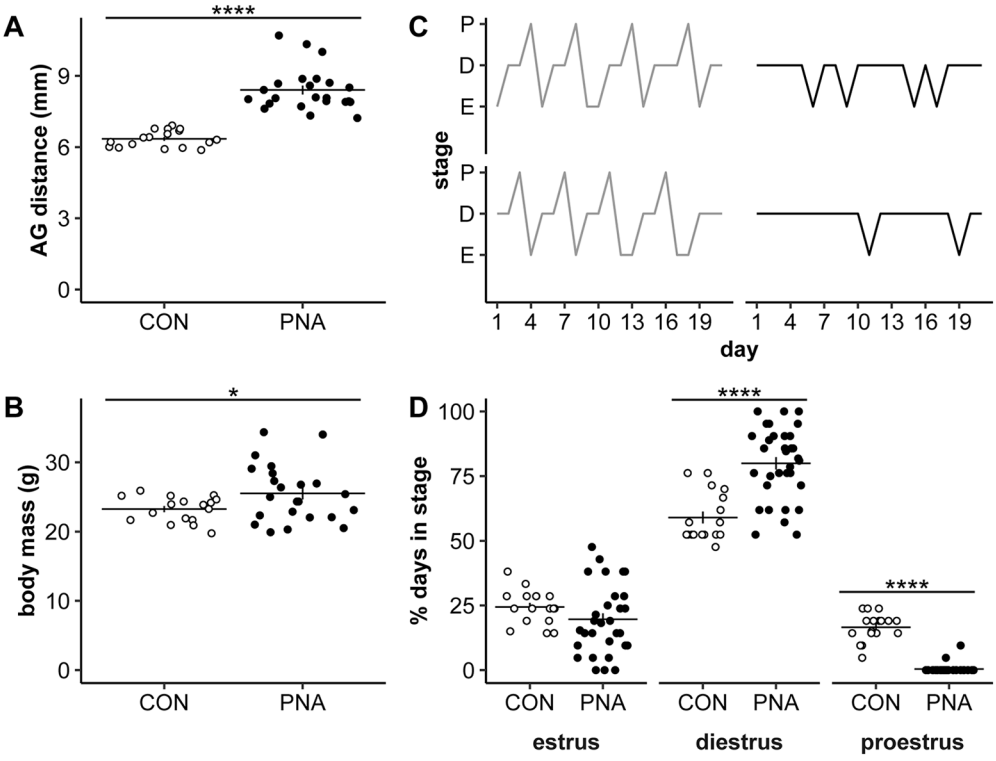

Figure 1. Confirmation of PNA phenotype in adults and surviving littermates of 3wk-old mice used for electrophysiology. ***A***, ***B***, ***D***, Individual values (CON open symbols, PNA black symbols) and mean ± SEM for anogenital (AG) distance (***A***), body mass (***B***), or percent days in each cycle stage (***D***). ***C***, Representative estrous cycles over a 3wk period; P, proestrus; D, diestrus; E, estrus. CON are shown on the left in grey, and PNA are on the right in black. Statistical parameters reported in Table 2; $^{*}p < 0.05$, $^{****}p \leq 0.0001$.

exhibited firing patterns consistent with episodic activity (representative traces in Fig. 2*A*,*B*). About half of recorded Tac2-GFP neurons were quiescent (defined as <0.005 Hz). The proportion of quiescent neurons did not vary with age or treatment (Fig. 2*C*; Breslow-Day test for independence and Mantel-Haenszel χ^2 test (Simonoff, 2003) statistical parameters reported in Table 3; 3wk-CON $n = 11$ cells from 7 mice in 5 litters, 3wk-PNA $n = 22$ cells from 12 mice in 6 litters, adult-CON $n = 15$ cells from 10 mice in 6 litters, adult-PNA $n = 22$ cells from 13 mice in 8 litters). Neither age nor PNA treatment affected the mean firing frequency of Tac2-GFP neurons over the recording period (Fig. 2*D*).

Figure 2 includes cells that were quiescent; quiescence is likely an important part of the biology of these cells given their postulated role as a component of the GnRH pulse generator. It is possible that either PNA treatment or development modify the degree of firing during active periods. When the firing frequency of just the spontaneously active (≥0.005 Hz) cells is compared, however, there were still no differences (two-way interaction: $F_{(1,29)} = 0.351$, $p = 0.558$; effect of treatment: $F_{(1,29)} = 0.183$, $p = 0.672$;

Table 2: Statistical parameters characterizing the PNA phenotype (Fig. 1)

Property	Two-tailed unpaired Welch-corrected Student's *t* test	Mean difference	Effect size, Cohen's *d*		
Anogenital distance (mm)	$t_{(30.13)} = 10.052$, **$p < 0.0001$**	Diff 2.06 [CI 1.64, 2.48]	$d = 3.03$		
Body mass (g)	$t_{(32.03)} = 2.331$, **$p = 0.0262$**	Diff 2.26 [CI 0.29, 4.24]	$d = 0.707$		
Property	**χ^2 test**		**Estrus**	**Diestrus**	**Proestrus**
Estrous cycle stage distribution	$\chi^2 = 111.392$, $n = 992$, df = 2, **$p < 0.0001$**	Std resid: Fisher's exact test; Bonferroni adjusted:	−1.79 $p = 0.226$	7.08 **$p < 0.0001$**	10.11 **$p < 0.0001$**

Bold indicates $p < 0.05$. Std resid, standardized residuals of PNA group from χ^2 test.

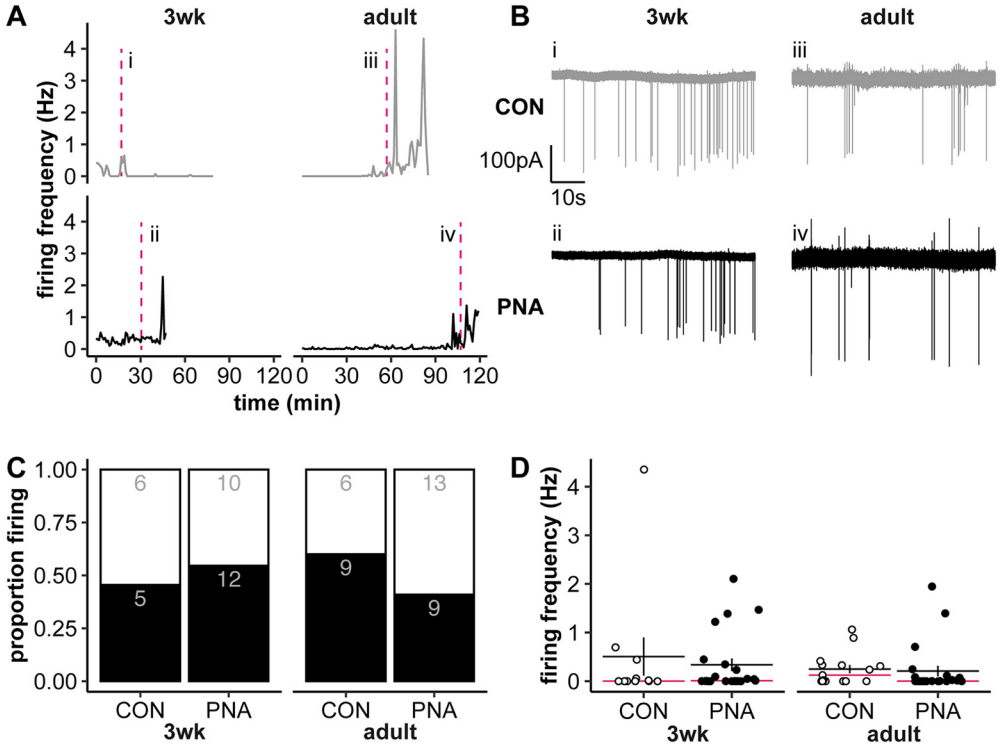

Figure 2. Effect of age and PNA treatment on KNDy neuron firing activity. ***A***, Representative long-term firing patterns (1-min bins). CON are shown on the top in gray, PNA on the bottom in black for each age. The time of the traces shown in ***B*** is designated by the magenta dashed lines in panel ***A***. ***B***, Examples of raw firing data (60 s) from the areas indicated in ***A***, details as in ***A***. The selected 60-s bins are representative of the mean firing rate of each group. ***C***, Proportion of cells with a firing frequency >0.005 Hz (black bars) versus <0.005 Hz (white bars); numbers are cell counts in each group. ***D***, Individual values (CON open symbols, PNA black symbols) and mean ± SEM and median (magenta line) for firing frequency across the duration of long-term recordings. Statistical parameters reported in Table 3.

effect of age: $F_{(1,29)} = 2.460$, $p = 0.128$). Of note, the variation in firing rate for cells recorded from the same mouse is similar to that observed when all data are considered. Specifically, for the 24 mice from which two or three cells were recorded, the mean difference in firing rate between the maximum and minimum firing cells was 0.53 Hz (±0.20 Hz; median: 0.19 Hz), and the mean coefficient of variance for the firing rate of cells from the same mouse was 94.8% (±15.9%; median: 71.0%). Thus, using multiple cells from an animal does not artificially lower variance, nor is the variation in firing rate observed fully attributed to individual variation.

Response to senktide

To verify viability of quiescent cells, the neurokinin-3 receptor agonist senktide was added at the conclusion of a subset of spontaneous recordings (3wk-CON $n = 8$ cells from 6 mice in 5 litters, 3wk-PNA $n = 12$ cells from 8 mice in 4 litters, adult-CON $n = 8$ cells from 6 mice in 3 litters, adult-PNA $n = 14$ cells from 10 mice in 6 litters). Only cells with spontaneous activity or action currents following senktide addition were included in the dataset. While performed as a quality check, this test is also biologically relevant as senktide activates firing activity of Tac2-GFP neurons (Ruka et al., 2013), and it is possible that age and

Table 3: Statistical parameters for firing activity (Fig. 2)

Parameter	Breslow–Day test for independence	Mantel–Haenszel χ^2	
Proportion firing	$\chi^2 = 1.285$, df = 1, $p = 0.257$	$\chi^2 = 0.069$, df = 1, $p = 0.7932$	
Parameter	**Age**	**PNA treatment**	**Interaction**
Firing frequency	Diff −0.193 [CI −0.537, 0.151] $F_{(1,66)} = 1.251$; $p = 0.267$	Diff −0.104 [CI −0.448, 0.240] $F_{(1,66)} = 0.362$; $p = 0.549$	Diff 0.130 [CI −0.558, 0.819] $F_{(1,66)} = 0.143$; $p = 0.707$

Independence of treatment and age with firing proportion was assessed with Breslow–Day test. This was followed by the Mantel–Haenszel χ^2 test with continuity correction to determine the effect of treatment on firing proportion when controlling for age (Simonoff, 2003). A two-way ANOVA was conducted for firing frequency.

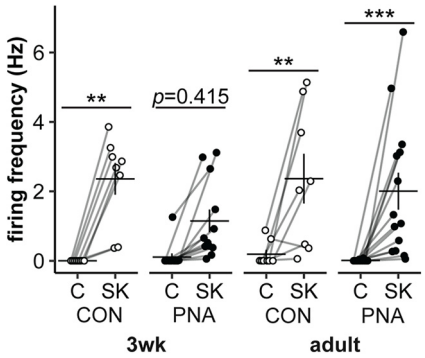

Figure 3. Senktide activates KNDy neuron firing activity. Individual values and mean ± SEM of firing rate during 5-min control (C) and senktide (SK) periods. CON mice are shown in open symbols, PNA mice in black symbols; $^{**}p \leq 0.01$, $^{***}p \leq 0.001$. Statistical parameters in Table 4.

treatment alter this. Tac2-GFP neurons responded to senktide with an increase in firing frequency (Fig. 3; statistical parameters in Table 4, main effect of time, $p < 0.0001$). This increase was evident in adult-CON ($p = 0.007$), adult-PNA ($p = 0.001$), and 3wk-CON ($p = 0.003$), yet there was not a significant increase for the 3wk-PNA ($p = 0.415$). This suggests that PNA treatment may alter the development of the response to senktide in KNDy neurons.

Short-term firing pattern

Examining the average firing frequency over the duration of the recording could obscure changes in the short-term organization of action potentials that may be more relevant for neurosecretion (Cazalis et al., 1985; Dutton and Dyball, 1979). We thus investigated the effect of age and PNA treatment on short-term firing patterns called bursts. (Fig. 4; statistical parameters in Table 5). Because not all cells exhibit burst firing, the n for cells changes for parts B, C, and D, and for part F as detailed in the legend. There were no differences because of age or treatment on any parameter other than burst duration. Burst duration was greater in cells from adults than those from 3wk-old mice (Fig. 4*B*, $p = 0.031$). An increase in burst duration could occur as a result of more spikes per burst, and/or a longer intraburst interval. Although it did not reach the level set for statistical significance, the increase in burst duration in adults appears to be driven primarily by increased spikes per burst (Fig. 4*C*, $p = 0.096$) rather than a change in the intraburst interval (Fig. 4*D*, $p = 0.911$).

Development but not PNA affects expression of key transcripts

To examine the effects of age and PNA on steroid receptors and KNDy neuron peptides and receptors in the arcuate nucleus, we quantified mRNA expression of androgen (*Ar*), estrogen (*Esr1*), and progesterone (*Pgr*) receptors and of kisspeptin (*Kiss1*), neurokinin B (*Tac2*), and dynorphin (*Pdyn*), and their corresponding receptors (*Kiss1r*, *Tacr3*, and *Oprk1*, respectively). *Tac2* ($p = 0.0001$) and *Tacr3* ($p < 0.0001$) expression were both increased in adults compared with 3wk-old mice (Fig. 5, statistical parameters in Table 6; 3wk-CON $n = 9$ mice, 3wk-PNA $n = 8$ mice, adult-CON $n = 8$ mice, adult-PNA $n = 7$ mice). Similarly, *Ar* ($p < 0.0001$) and *Pgr* ($p < 0.0001$) were increased in the adult arcuate nucleus (Fig. 5). PNA treatment did not alter expression of any transcripts, although there were weak trends for PNA to increase expression of *Kiss1r* ($p = 0.091$) and *Pdyn* ($p = 0.071$; Fig. 5).

Table 4: Statistical parameters from three-way mixed model ANOVA assessing the effect of age and PNA treatment on the KNDy cell response to senktide (Fig. 3)

Effect	Statistic	Generalized η^2
Senktide	$F_{(1,38)} = 52.35$, $p < 0.0001$	0.395
Age	$F_{(1,38)} = 0.7515$, $p = 0.391$	0.010
PNA treatment	$F_{(1,38)} = 2.235$, $p = 0.143$	0.030
Senktide × age	$F_{(1,38)} = 0.5459$, $p = 0.465$	0.007
Senktide × PNA treatment	$F_{(1,38)} = 2.051$, $p = 0.160$	0.025
Age × treatment	$F_{(1,38)} = 0.2633$, $p = 0.611$	0.004
Senktide × age × PNA treatment	$F_{(1,38)} = 1.179$, $p = 0.284$	0.015
Bonferroni's multiple comparisons test	**Mean diff (Hz), 95% CI of diff**	**Statistic**
SK 3wk-CON – C 3wk-CON	Diff 2.36, [CI 0.59, 4.13]	$t_{(38)} = 4.055$, $\mathbf{p = 0.003}$
SK 3wk-PNA – C 3wk-PNA	Diff 1.04, [CI −0.41, 2.49]	$t_{(38)} = 2.192$, $p = 0.415$
SK adult-CON – C adult-CON	Diff 2.178, [CI 0.40, 3.95]	$t_{(38)} = 3.743$, $\mathbf{p = 0.007}$
SK adult-PNA – C adult-PNA	Diff 2.00, [CI 0.66, 3.34]	$t_{(38)} = 4.540$, $\mathbf{p = 0.001}$
C 3wk-PNA – C 3wk-CON	Diff 0.11, [CI −1.51, 1.72]	$t_{(76)} = 0.194$, $p > 0.999$
C adult-PNA – C adult-CON	Diff −0.18, [CI −1.75, 1.39]	$t_{(76)} = 0.340$, $p > 0.999$
SK 3wk-PNA – SK 3wk-CON	Diff −1.21, [CI −2.82, 0.40]	$t_{(76)} = 2.223$, $p = 0.350$
SK adult-PNA – SK adult-CON	Diff −0.36, [CI −1.93, 1.20]	$t_{(76)} = 0.682$, $p > 0.999$
C adult-CON – C 3wk-CON	Diff 0.19, [CI −1.58, 1.95]	$t_{(76)} = 0.315$, $p > 0.999$
C adult-PNA – C 3wk-PNA	Diff −0.10, [CI −1.49, 1.29]	$t_{(76)} = 0.207$, $p > 0.999$
SK adult-CON – SK 3wk-CON	Diff 0.01, [CI −1.76, 1.77]	$t_{(76)} = 0.011$, $p > 0.999$
SK adult-PNA – SK 3wk-PNA	Diff 0.86, [CI −0.53, 2.25]	$t_{(76)} = 1.825$, $p = 0.863$

The effect size, generalized η^2, is reported for each effect. Bonferroni multiple comparisons for cells that differ by only one factor. Bold indicates $p < 0.05$.

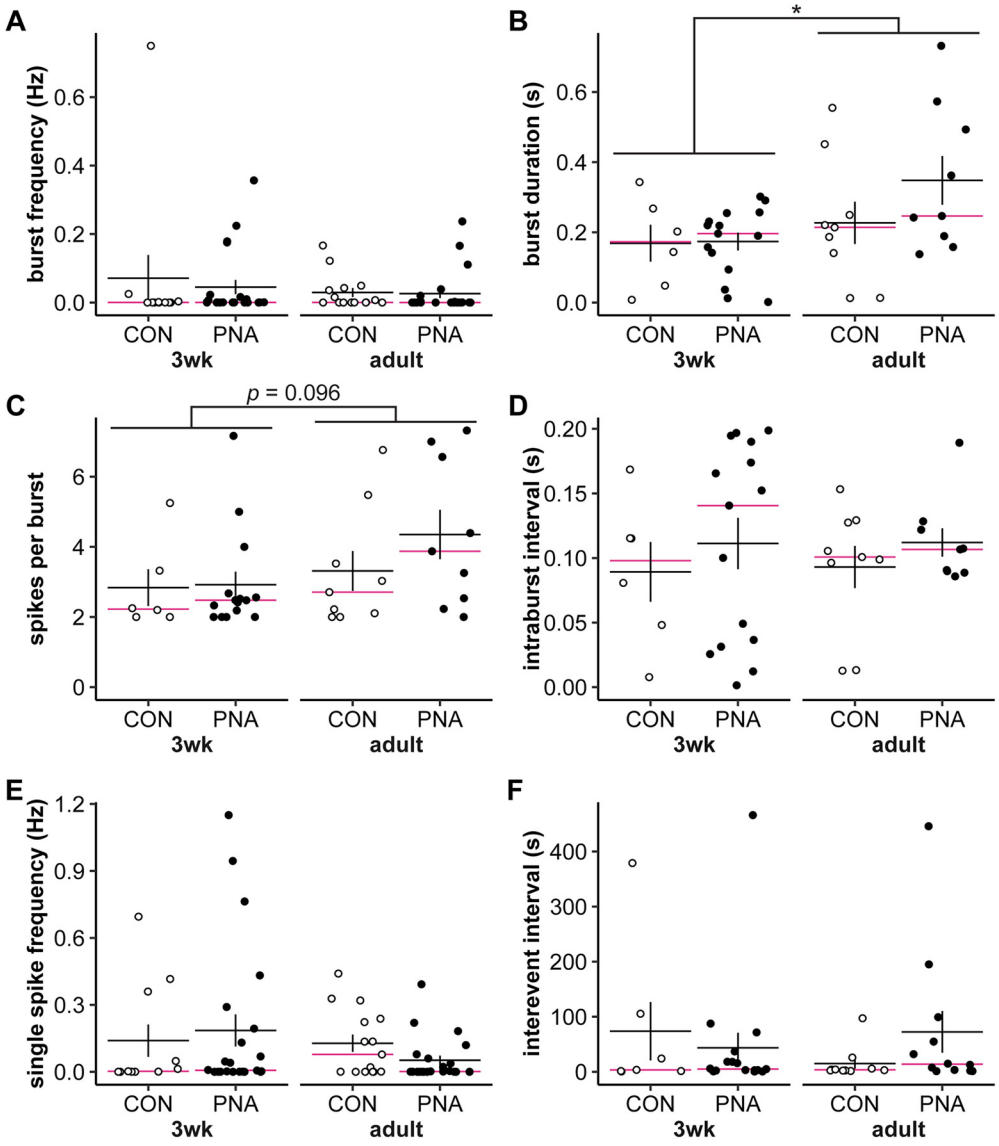

Figure 4. Effect of age and PNA treatment on burst parameters. ***A–F***, Individual values (CON open symbols, PNA black symbols) and mean ± SEM and median (magenta lines) for burst frequency (***A***), burst duration (***B***), spikes per burst (***C***), intraburst interval (***D***), single spike frequency (***E***), and interevent interval (***F***). ***B–D***, Burst parameters are only calculated for cells with at least one burst; 3wk-CON $n = 6$ cells from 5 mice in 4 litters, 3wk-PNA $n = 15$ cells from 10 mice in 5 litters, adult-CON $n = 9$ cells from 8 mice in 5 litters, adult-PNA $n = 9$ cells from 8 mice in 5 litters. ***F***, Calculating interevent interval also requires multiple events, 3wk-CON $n = 7$ cells from 6 mice in 5 litters, 3wk-PNA $n = 17$ cells from 10 mice in 5 litters, adult-CON $n = 10$ cells from 10 mice in 6 litters, adult-PNA $n = 12$ cells from 9 mice in 5 litters; $^*p < 0.05$. Statistical parameters in Table 5.

Discussion

Changes in the frequency of GnRH release throughout female reproductive cycles are important for fertility. Patients with PCOS often fail to exhibit these changes, instead displaying a persistently elevated LH, and presumably GnRH, pulse frequency. Here, we tested the hypothesis that prenatal exposure to elevated androgens, a model that recapitulates aspects of PCOS, disrupts the hypothalamo-pituitary-gonadal axis in part by changing the firing activity of KNDy neurons in the arcuate nucleus. Contrary to our hypothesis, neither overall spontaneous activity of KNDy neurons nor most burst characteristics were altered by PNA treatment either before puberty or in adulthood. Expression of *Tac2*, *Tacr3*, *Ar*, and *Pgr* mRNA was greater in the arcuate of adult mice as compared with 3wk-old mice, but this expression was not impacted by PNA treatment. These findings suggest that changes in KNDy neuron activity alone are not responsible for the altered LH pulse frequency observed with PNA treatment.

KNDy neurons have been postulated to be the pulse generator for GnRH release (Clarkson et al., 2017; McQuillan et al., 2019). Kisspeptin increases GnRH release (Messager et al., 2005; Glanowska et al., 2014) *in vivo* and in brain slices, and increases GnRH neuron activity (Han et al., 2005; Pielecka-Fortuna et al., 2008) in brain slices. As the putative pulse generator, KNDy neuron

Table 5: Two-way ANOVA statistical parameters for burst parameters

Property	Age	PNA treatment	Interaction
Burst frequency	Diff −0.030	Diff −0.014	Diff 0.023
	[CI −0.086, 0.025]	[CI −0.070, 0.041]	[CI −0.088, 0.134]
	$F_{(1,66)} = 1.184$; $p = 0.281$	$F_{(1,66)} = 0.267$; $p = 0.608$	$F_{(1,66)} = 0.167$; $p = 0.684$
Burst duration	Diff 0.116	Diff 0.063	Diff 0.116
	[CI 0.011, 0.221]	[CI −0.042, 0.168]	[CI −0.94, 0.326]
	$F_{(1,35)} = 5.068$; $\mathbf{p = 0.031}$	$F_{(1,35)} = 1.479$; $p = 0.232$	$F_{(1,35)} = 1.263$; $p = 0.269$
Spikes per burst	Diff 0.954	Diff 0.560	Diff 0.955
	[CI −0.178, 2.087]	[CI −0.572, 1.693]	[CI −1.310, 3.220]
	$F_{(1,35)} = 2.927$; $p = 0.096$	$F_{(1,35)} = 1.009$; $p = 0.322$	$F_{(1,35)} = 0.733$; $p = 0.398$
Intraburst interval	Diff 0.002	Diff 0.021	Diff −0.003
	[CI −0.039, 0.044]	[CI −0.021, 0.062]	[CI −0.085, 0.079]
	$F_{(1,35)} = 0.013$; $p = 0.911$	$F_{(1,35)} = 1.021$; $p = 0.319$	$F_{(1,35)} = 0.005$; $p = 0.942$
Single spike frequency	Diff −0.073	Diff −0.015	Diff −0.122
	[CI −0.187, 0.041]	[CI −0.129, 0.099]	[CI −0.350, 0.106]
	$F_{(1,66)} = 1.63$; $p = 0.206$	$F_{(1,66)} = 0.072$; $p = 0.790$	$F_{(1,66)} = 1.147$; $p = 0.288$
Interburst interval	Diff −14.87	Diff 13.72	Diff 87.73
	[CI −84.09, 54.36]	[CI −55.51, 82.94]	[CI −50.71, 226.2]
	$F_{(1,42)} = 0.188$; $p = 0.667$	$F_{(1,42)} = 0.160$; $p = 0.691$	$F_{(1,42)} = 1.635$; $p = 0.208$

Bold indicates $p < 0.05$.

activity would be expected to change in manners that reflect the output of GnRH neurons and LH release. GnRH neuron firing rate changes with development and PNA treatment alters the typical developmental trajectory. Specifically, in GnRH neurons from adults, firing rate is elevated in PNA mice (Roland and Moenter, 2011), whereas firing frequency in cells from PNA mice before puberty at 3wks of age is reduced, because PNA treatment blunts the typical peak in firing that occurs near this age in control mice (Dulka and Moenter, 2017). We expected similar effects in KNDy neurons. Consistent with prior studies in adults, many of the KNDy cells that we recorded were quiescent (de Croft et al., 2012; Frazão et al., 2013; Ruka et al., 2013). Surprisingly, neither age nor PNA treatment

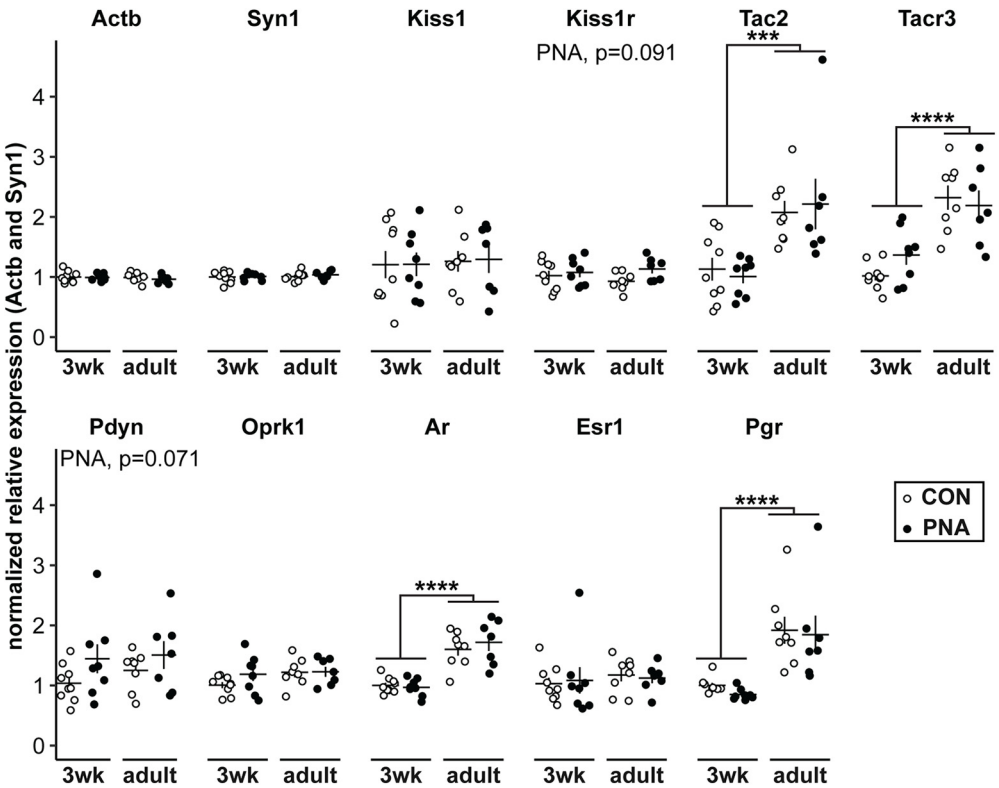

Figure 5. Effect of age and PNA treatment on arcuate nucleus mRNA transcripts. Individual values (CON open symbols, PNA black symbols) and mean ± SEM for *Actb*, *Syn1*, *Kiss1*, *Kiss1r*, *Tac2*, *Tacr3*, *Pdyn*, *Oprk1*, *Ar*, *Esr1*, and *Pgr* mRNA isolated from arcuate nucleus tissue punches. Statistical parameters are reported in Table 6; ***$p \leq 0.001$, ****$p \leq 0.0001$.

Table 6: Two-way ANOVA statistical parameters for arcuate mRNA expression

Transcript	Age	PNA treatment	Interaction
Actb	Diff −0.018	Diff −0.019B2	Diff −0.019
	[CI −0.074, 0.038]	[CI −0.074, 0.037]	[CI −0.131, 0.092]
	$F_{(1,28)} = 0.436$; $p = 0.515$	$F_{(1,28)} = 0.466$; $p = 0.501$	$F_{(1,28)} = 0.126$; $p = 0.725$
Syn1	Diff 0.018	Diff 0.019	Diff 0.019
	[CI −0.038, 0.074]	[CI −0.037, 0.074]	[CI −0.092, 0.131]
	$F_{(1,28)} = 0.436$; $p = 0.515$	$F_{(1,28)} = 0.466$; $p = 0.501$	$F_{(1,28)} = 0.126$; $p = 0.725$
Kiss1	Diff 0.068	Diff 0.019	Diff 0.028
	[CI −0.358, 0.495]	[CI −0.407, 0.445]	[CI −0.824, 0.880]
	$F_{(1,28)} = 0.108$; $p = 0.744$	$F_{(1,28)} = 0.009$; $p = 0.926$	$F_{(1,28)} = 0.004$; $p = 0.947$
Kiss1r	Diff −0.019	Diff 0.129	Diff 0.150
	[CI −0.170, 0.132]	[CI −0.022, 0.280]	[CI −0.152, 0.453]
	$F_{(1,28)} = 0.068$; $p = 0.796$	$F_{(1,28)} = 3.062$; $p = 0.091$	$F_{(1,28)} = 1.038$; $p = 0.317$
Tac2	Diff 1.075	Diff 0.009	Diff 0.264
	[CI 0.584, 1.566]	[CI −0.482, 0.500]	[CI −0.718, 1.245]
	$F_{(1,28)} = 20.113$; $\mathbf{p = 0.0001}$	$F_{(1,28)} = 0.001$; $p = 0.97$	$F_{(1,28)} = 0.302$; $p = 0.587$
Tacr3	Diff 1.064	Diff 0.108	Diff −0.476
	[CI 0.707, 1.420]	[CI −0.249, 0.464]	[CI −1.189, 0.238]
	$F_{(1,28)} = 37.321$; $\mathbf{p < 0.0001}$	$F_{(1,28)} = 0.381$; $p = 0.542$	$F_{(1,28)} = 1.865$; $p = 0.183$
Pdyn	Diff 0.138	Diff 0.331	Diff −0.153
	[CI −0.224, 0.499]	[CI −0.030, 0.693]	[CI −0.876, 0.571]
	$F_{(1,28)} = 0.608$; $p = 0.442$	$F_{(1,28)} = 3.520$; $p = 0.071$	$F_{(1,28)} = 0.187$; $p = 0.669$
Opkr1	Diff 0.127	Diff 0.095	Diff −0.170
	[CI −0.044, 0.298]	[CI −0.076, 0.266]	[CI −0.512, 0.172]
	$F_{(1,28)} = 2.313$; $p = 0.139$	$F_{(1,28)} = 1.294$; $p = 0.265$	$F_{(1,28)} = 1.033$; $p = 0.318$
Ar	Diff 0.673	Diff 0.041	Diff 0.150
	[CI 0.493, 0.854]	[CI −0.140, 0.221]	[CI −0.212, 0.511]
	$F_{(1,28)} = 58.323$; $\mathbf{p < 0.0001}$	$F_{(1,28)} = 0.215$; $p = 0.647$	$F_{(1,28)} = 0.720$; $p = 0.403$
Esr1	Diff 0.091	Diff 0.002	Diff −0.105
	[CI −0.195, 0.377]	[CI −0.284, 0.288]	[CI −677, 0.467]
	$F_{(1,28)} = 0.428$; $p = 0.519$	$F_{(1,28)} = 0.0002$; $p = 0.989$	$F_{(1,28)} = 0.141$; $p = 0.71$
Pgr	Diff 0.955	Diff −0.114	Diff 0.076
	[CI 0.585, 1.325]	[CI −0.484, 0.257]	[CI −0.664, 0.817]
	$F_{(1,28)} = 27.92$; $\mathbf{p < 0.0001}$	$F_{(1,28)} = 0.395$; $p = 0.535$	$F_{(1,28)} = 0.045$; $p = 0.834$

Bold indicates $p < 0.05$.

altered the mean firing frequency of KNDy neurons. Similarly, effects on short-term burst firing were minimal. These observations suggest that both development and prenatal exposure to androgens alter GnRH neuron activity and release via mechanisms other than changing the activity of KNDy neurons.

The elevated LH pulse frequency in patients with PCOS is attributable at least in part to reduced negative feedback actions of progesterone (Pastor et al., 1998). When patients are treated with the anti-androgen flutamide, the suppressive effects of progesterone on LH release are partially restored (Eagleson et al., 2000), suggesting that hyperandrogenism plays a role in this impaired negative feedback. The opposing effects of androgens and progestins is supported by findings in murine brain slices that androgens interfere with progesterone negative feedback on GnRH neuron firing rate (Pielecka et al., 2006) and GABA transmission to these cells (Sullivan and Moenter, 2005). The elevated LH pulse frequency in PNA mice (Moore et al., 2015) may have a similar origin to that in patients with PCOS. Following ovariectomy, LH levels rise in control mice and to a lesser extent in PNA mice (Moore et al., 2015). Administration of progesterone reduces the LH levels in ovariectomized control but not PNA mice, indicative of impaired negative feedback in the latter (Moore et al., 2015). Progesterone may act in part through receptors in the arcuate nucleus to reduce LH pulse frequency, as administration of progesterone receptor antagonists in this brain region reduces the interval between LH pulses following intraperitoneal injection of progesterone (He et al., 2017). Progesterone also reduces the frequency of peaks in KNDy neuron activity measured by GCaMP fluorescence that are correlated with LH release (McQuillan et al., 2019), but whether or not this is a direct effect on KNDy neurons is not known.

A possible alternative mediator of central changes in PNA mice is GABAergic neurons. A subset of KNDy neurons may be GABAergic, although estimates vary on the percentage; up to 50% of KNDy neurons express GAD67 (Cravo et al., 2011), but only ~10–15% of KNDy neurons co-express the vesicular GABA transporter VGaT (Marshall et al., 2017). PNA treatment increases the frequency of GABAergic postsynaptic currents recorded in GnRH neurons from both adult and prepubertal 3wk-old mice (Sullivan and Moenter, 2004; Berg et al., 2018), which given the excitatory effects of GABA in GnRH neurons can contribute to increased activity. At least some of this increased transmission appears to arise from the arcuate nucleus as appositions between GABAergic neurons in the region and GnRH neurons increase in PNA mice (Moore et al.,

2015). Consistent with an involvement in the steroid feedback effects discussed above, PNA treatment reduces the expression of progesterone receptors in GABAergic neurons in the arcuate nucleus (Moore et al., 2015). High-frequency optogenetic stimulation of GABAergic neurons in the arcuate nucleus can stimulate LH release in control mice (Silva et al., 2019). Longer-term chemogenetic activation of these GABAergic neurons also increases LH release, disrupts estrous cycles and decreases the number of corpora lutea (Silva et al., 2019). Together, these results point to GABAergic neurons in the arcuate as a potential steroid-sensitive mediator of PNA treatment on GnRH neuron activity.

It is important to point out that our findings do not rule out a possible role of KNDy neurons in modulating the effects of PNA or age on GnRH and LH release. KNDy neurons are part of an intricate network in the arcuate nucleus, and they project to GnRH distal projections in the median eminence (Yip et al., 2015). In rats, PNA increases the number of arcuate cells immunopositive for kisspeptin and neurokinin B (Osuka et al., 2017) and the relative levels of kisspeptin and neurokinin B mRNA (Yan et al., 2014). In sheep, prenatal testosterone treatment reduced the number of putatively inhibitory dynorphin-immunopositive cells without changing the number of kisspeptin-immunopositive cells in the arcuate nucleus (Cheng et al., 2010). In contrast, following 7 d of estradiol treatment, PNA mice did not differ in the relative mRNA expression of KNDy neuron peptides or receptors in the arcuate nucleus (Caldwell et al., 2015). Similarly, we only observed developmental changes in KNDy neuron peptide and receptor mRNA expression in the arcuate nucleus, but no changes because of PNA treatment. The variation between studies may be attributable to animal models or the examination of mRNA versus peptide.

Prenatal testosterone exposure also alters synaptic connections of KNDy neurons with one another and projections to GnRH neurons (Cernea et al., 2015). It remains possible that even without a change in firing frequency, PNA may alter the amount of kisspeptin and/or other neuromodulators released at a given level of activity, potentially leading to increased GnRH release. The reciprocal connections of the network of KNDy neurons are also thought to be important for their involvement in GnRH pulse regulation, and PNA could alter these dynamics. Neurokinin B increases and dynorphin decreases the activity of KNDy neurons (de Croft et al., 2012, 2013; Ruka et al., 2013), whereas kisspeptin does not affect the firing frequency of other KNDy neurons (de Croft et al., 2013). The effects of neurokinin B and dynorphin signaling are modulated by steroidal milieu (Ruka et al., 2016). Although we did not observe effects of PNA on mRNA expression within the whole arcuate nucleus, our study does not address the possibility that gene expression, including that of receptors for KNDy peptides, may be altered specifically within KNDy neurons. Intriguingly, in the present study, senktide, a neurokinin-3 receptor agonist, was less effective at eliciting an increase in firing frequency of KNDy neurons from 3wk-old PNA mice. This suggests that PNA disrupts the development of this network.

A key feature of patients with PCOS is a persistently elevated LH pulse frequency that is most similar to the mid-to-late follicular phase (McCartney et al., 2002). Although we often recorded cells for at least 60 min, these recordings were not of sufficient length to characterize rigorously the frequency and duration of peaks and nadirs in firing activity. It is plausible that the firing activity of KNDy neurons during a peak in activity does not differ with age or PNA treatment, but that the frequency of these peaks may be increased in adult-PNA mice, leading to the elevated GnRH and LH pulse frequency. In this regard, the frequency of peaks, but not mean firing rate, was altered in KNDy neurons from adult males by orchidectomy and steroid replacement (Vanacker et al., 2017). Because PNA mice fail to exhibit typical estrous cycles and remain persistently in a diestrus-like state based on vaginal cytology, we specifically compared their firing frequency to that of cells from diestrous control mice. The frequency of peaks in calcium activity of KNDy neurons across the estrous cycle was not different from metestrus to diestrus to proestrus (McQuillan et al., 2019). In contrast, KNDy cells from mice in estrus exhibited a markedly decreased frequency of these peaks, postulated to be due in part to the negative feedback effects of progesterone (McQuillan et al., 2019). It is thus possible that a difference in firing rate of KNDy neurons would be observed on estrus that could be attributable to impaired progesterone negative feedback in adult-PNA mice. Our choice to record on diestrus was based not only on the practical consideration that PNA mice are often in persistent diestrus, but also on the observed increase in LH pulse frequency in PNA mice during this stage (Moore et al., 2015). The lack of difference in KNDy neuron firing rate in the present study thus supports the postulate that this increased episodic LH release arises from other cells, or is disrupted by the brain slice preparation.

The work presented here indicates that the elevated GnRH neuron firing frequency and LH pulse frequency associated with PNA cannot be solely explained by changes in arcuate KNDy neuron firing frequency or bursting patterns. PNA may also alter the development of the stimulatory effects of neurokinin-3 receptor activation on KNDy neuron activity, disrupting network dynamics. Our work points to the importance of the broader network of neurons within the hypothalamus, including GABAergic cells, as mediators of the effects of hyperandrogenism on the output of the hypothalamic-pituitary-gonadal axis.

References

Abbott DH, Barnett DK, Levine JE, Padmanabhan V, Dumesic DA, Jacoris S, Tarantal AF (2008) Endocrine antecedents of polycystic ovary syndrome in fetal and infant prenatally androgenized female rhesus monkeys. Biol Reprod 79:154–163.

Abbott DH, Rayome BH, Dumesic DA, Lewis KC, Edwards AK, Wallen K, Wilson ME, Appt SE, Levine JE (2017) Clustering of PCOS-like traits in naturally hyperandrogenic female rhesus monkeys. Hum Reprod 32:923–936.

Abbott DH, Rogers J, Dumesic DA, Levine JE (2019) Naturally occurring and experimentally induced rhesus macaque models for polycystic ovary syndrome: translational gateways to clinical application. Med Sci 7:107.

Alcami P, Franconville R, Llano I, Marty A (2012) Measuring the firing rate of high-resistance neurons with cell-attached recording. J Neurosci 32:3118–3130.
Berg T, Silveira MA, Moenter SM (2018) Prepubertal development of GABAergic transmission to gonadotropin-releasing hormone (GnRH) neurons and postsynaptic response are altered by prenatal androgenization. J Neurosci 38:2283–2293.
Birch RA, Padmanabhan V, Foster DL, Unsworth WP, Robinson JE (2003) Prenatal programming of reproductive neuroendocrine function: fetal androgen exposure produces progressive disruption of reproductive cycles in sheep. Endocrinology 144:1426–1434.
Bustin S (2002) Quantification of mRNA using real-time reverse transcription PCR (RT-PCR): trends and problems. J Mol Endocrinol 29:23–39.
Caldwell ASL, Eid S, Kay CR, Jimenez M, McMahon AC, Desai R, Allan CM, Smith JT, Handelsman DJ, Walters KA (2015) Haplosufficient genomic androgen receptor signaling is adequate to protect female mice from induction of polycystic ovary syndrome features by prenatal hyperandrogenization. Endocrinology 156:1441–1452.
Caldwell ASL, Edwards MC, Desai R, Jimenez M, Gilchrist RB, Handelsman DJ, Walters KA (2017) Neuroendocrine androgen action is a key extraovarian mediator in the development of polycystic ovary syndrome. Proc Natl Acad Sci USA 114:E3334–E3343.
Cazalis M, Dayanithi G, Nordmann JJ (1985) The role of patterned burst and interburst interval on the excitation-coupling mechanism in the isolated rat neural lobe. J Physiol 369:45–60.
Cernea M, Padmanabhan V, Goodman RL, Coolen LM, Lehman MN (2015) Prenatal testosterone treatment leads to changes in the morphology of KNDy neurons, their inputs, and projections to GnRH cells in female sheep. Endocrinology 156:3277–3291.
Chang W (2014) extrafont: tools for using fonts (R package version 0.17). Available at https://cran.r-project.org/package=extrafont.
Chang W, Cheng J, Allaire J, Xie Y, McPherson J (2020) shiny: web application framework for R (R package version 1.5.0). Available at https://cran.r-project.org/package=shiny.
Cheng G, Coolen LM, Padmanabhan V, Goodman RL, Lehman MN (2010) The kisspeptin/neurokinin B/dynorphin (KNDy) cell population of the arcuate nucleus: sex differences and effects of prenatal testosterone in sheep. Endocrinology 151:301–311.
Clarkson J, Han SY, Piet R, McLennan T, Kane GM, Ng J, Porteous RW, Kim JS, Colledge WH, Iremonger KJ, Herbison AE (2017) Definition of the hypothalamic GnRH pulse generator in mice. Proc Natl Acad Sci USA 114:E10216–E10223.
Cravo RM, Margatho LO, Osborne-Lawrence S, Donato J, Atkin S, Bookout AL, Rovinsky S, Frazão R, Lee CE, Gautron L, Zigman JM, Elias CF (2011) Characterization of Kiss1 neurons using transgenic mouse models. Neuroscience 173:37–56.
de Croft S, Piet R, Mayer C, Mai O, Boehm U, Herbison AE (2012) Spontaneous kisspeptin neuron firing in the adult mouse reveals marked sex and brain region differences but no support for a direct role in negative feedback. Endocrinology 153:5384–5393.
de Croft S, Boehm U, Herbison AE (2013) Neurokinin B activates arcuate kisspeptin neurons through multiple tachykinin receptors in the male mouse. Endocrinology 154:2750–2760.
Dulka EA, Moenter SM (2017) Prepubertal development of gonadotropin-releasing hormone neuron activity is altered by sex, age, and prenatal androgen exposure. Endocrinology 158:3943–3953.
Dumesic DA, Abbott DH, Eisner JR, Goy RW (1997) Prenatal exposure of female rhesus monkeys to testosterone propionate increases serum luteinizing hormone levels in adulthood. Fertil Steril 67:155–163.
Dumesic DA, Oberfield SE, Stener-Victorin E, Marshall JC, Laven JS, Legro RS (2015) Scientific statement on the diagnostic criteria, epidemiology, pathophysiology, and molecular genetics of polycystic ovary syndrome. Endocr Rev 36:487–525.
Dutton A, Dyball RE (1979) Phasic firing enhances vasopressin release from the rat neurohypophysis. J Physiol 290:433–440.
Eagleson CA, Gingrich MB, Pastor CL, Arora TK, Burt CM, Evans WS, Marshall JC (2000) Polycystic ovarian syndrome: evidence that flutamide restores sensitivity of the gonadotropin-releasing hormone pulse generator to inhibition by estradiol and progesterone. J Clin Endocrinol Metab 85:4047–4052.
Foecking EM, Szabo M, Schwartz NB, Levine JE (2005) Neuroendocrine consequences of prenatal androgen exposure in the female rat: absence of luteinizing hormone surges, suppression of progesterone receptor gene expression, and acceleration of the gonadotropin-releasing hormone pulse generator. Biol Reprod 72:1475–1483.
Fox J, Weisberg S (2019) An {R} companion to applied regression, Ed 3. Thousand Oaks: SAGE Publications.
Frazão R, Cravo RM, Donato J, Ratra DV, Clegg DJ, Elmquist JK, Zigman JM, Williams KW, Elias CF (2013) Shift in Kiss1 cell activity requires estrogen receptor α. J Neurosci 33:2807–2820.
Glanowska KM, Burger LL, Moenter SM (2014) Development of gonadotropin-releasing hormone secretion and pituitary response. J Neurosci 34:15060–15069.
Gohel D (2020a) flextable: functions for tabular reporting (R package version 0.5.11). Available at https://cran.r-project.org/package=flextable.
Gohel D (2020b) officer: manipulation of Microsoft Word and PowerPoint documents (R package version 0.3.15). Available at https://cran.r-project.org/package=officer.
Haisenleder DJ, Dalkin AC, Ortolano GA, Marshall JC, Shupnik MA (1991) A pulsatile gonadotropin-releasing hormone stimulus is required to increase transcription of the gonadotropin subunit genes: evidence for differential regulation of transcription by pulse frequency in vivo. Endocrinology 128:509–517.
Han SK, Gottsch ML, Lee KJ, Popa SM, Smith JT, Jakawich SK, Clifton DK, Steiner RA, Herbison AE (2005) Activation of gonadotropin-releasing hormone neurons by kisspeptin as a neuroendocrine switch for the onset of puberty. J Neurosci 25:11349–11356.
Han SY, McLennan T, Czieselsky K, Herbison AE (2015) Selective optogenetic activation of arcuate kisspeptin neurons generates pulsatile luteinizing hormone secretion. Proc Natl Acad Sci USA 112:13109–13114.
He W, Li X, Adekunbi D, Liu Y, Long H, Wang L, Lyu Q, Kuang Y, O'Byrne KT (2017) Hypothalamic effects of progesterone on regulation of the pulsatile and surge release of luteinising hormone in female rats. Sci Rep 7:8096–8011.
Henry L, Wickham H (2020a) purrr: functional programming tools (R package version 0.3.4). Available at https://cran.r-project.org/package=purrr.
Henry L, Wickham H (2020b) rlang: functions for base types and core R and "tidyverse" features (R package version 0.4.8). Available at https://cran.r-project.org/package=rlang.
Herbison AE, Skinner DC, Robinson JE, King IS (1996) Androgen receptor-immunoreactive cells in ram hypothalamus: distribution and co-localization patterns with gonadotropin-releasing hormone, somatostatin and tyrosine hydroxylase. Neuroendocrinology 63:120–131.
Kassambara A (2020) ggpubr: "ggplot2" based publication ready plots (R package version 0.4.0). Available at https://cran.r-project.org/package=ggpubr.
Kassambara A (2021) rstatix: pipe-friendly framework for basic statistical tests (R package version 0.7.0). Available at https://cran.r-project.org/package=rstatix.
Levine JE, Ramirez VD (1982) Luteinizing hormone-releasing hormone release during the rat estrous cycle and after ovariectomy, as estimated with push-pull cannulae. Endocrinology 111:1439–1448.
Marshall CJ, Desroziers E, McLennan T, Campbell RE (2017) Defining subpopulations of arcuate nucleus GABA neurons in male, female, and prenatally androgenized female mice. Neuroendocrinology 105:157–169.
McCartney CR, Eagleson CA, Marshall JC (2002) Regulation of gonadotropin secretion: implications for polycystic ovary syndrome. Semin Reprod Med 20:317–326.
McQuillan HJ, Han SY, Cheong I, Herbison AE (2019) GnRH pulse generator activity across the estrous cycle of female mice. Endocrinology 160:1480–1491.

Messager S, Chatzidaki EE, Ma D, Hendrick AG, Zahn D, Dixon J, Thresher RR, Malinge I, Lomet D, Carlton MBL, Colledge WH, Caraty A, Aparicio SAJR (2005) Kisspeptin directly stimulates gonadotropin-releasing hormone release via G protein-coupled receptor 54. Proc Natl Acad Sci USA 102:1761–1766.

Moenter SM, Caraty A, Locatelli A, Karsch FJ (1991) Pattern of gonadotropin-releasing hormone (GnRH) secretion leading up to ovulation in the ewe: existence of a preovulatory GnRH surge. Endocrinology 129:1175–1182.

Moore AM, Prescott M, Marshall CJ, Yip SH, Campbell RE (2015) Enhancement of a robust arcuate GABAergic input to gonadotropin-releasing hormone neurons in a model of polycystic ovarian syndrome. Proc Natl Acad Sci USA 112:596–601.

Nunemaker CS, DeFazio RA, Moenter SM (2003) A targeted extracellular approach for recording long-term firing patterns of excitable cells: a practical guide. Biol Proced Online 5:53–62.

Oakley AE, Clifton DK, Steiner RA (2009) Kisspeptin signaling in the brain. Endocr Rev 30:713–743.

Osuka S, Iwase A, Nakahara T, Kondo M, Saito A, Nakamura T, Takikawa S, Goto M, Kotani T, Kikkawa F (2017) Kisspeptin in the hypothalamus of 2 rat models of polycystic ovary syndrome. Endocrinology 158:367–377.

Pastor CL, Griffin-Korf ML, Aloi JA, Evans WS, Marshall JC (1998) Polycystic ovary syndrome: evidence for reduced sensitivity of the gonadotropin-releasing hormone pulse generator to inhibition by estradiol and progesterone. J Clin Endocrinol Metab 83:582–590.

Pielecka-Fortuna J, Chu Z, Moenter SM (2008) Kisspeptin acts directly and indirectly to increase gonadotropin-releasing hormone neuron activity and its effects are modulated by estradiol. Endocrinology 149:1979–1986.

Pielecka J, Quaynor SD, Moenter SM (2006) Androgens increase gonadotropin-releasing hormone neuron firing activity in females and interfere with progesterone negative feedback. Endocrinology 147:1474–1479.

R Core Team (2019) R: a language and environment for statistical computing. R Foundation for Statistical Computing. Available at https://www.r-project.org/.

Roland AV, Moenter SM (2011) Prenatal androgenization of female mice programs an increase in firing activity of gonadotropin-releasing hormone (GnRH) neurons that is reversed by metformin treatment in adulthood. Endocrinology 152:618–628.

Rosenfield RL (2007) Identifying children at risk for polycystic ovary syndrome. J Clin Endocrinol Metab 92:787–796.

RStudio Team (2019) RStudio: integrated development environment for R. Available at http://www.rstudio.com/.

Ruka KA, Burger LL, Moenter SM (2013) Regulation of arcuate neurons coexpressing kisspeptin, neurokinin B, and dynorphin by modulators of neurokinin 3 and κ-opioid receptors in adult male mice. Endocrinology 154:2761–2771.

Ruka KA, Burger LL, Moenter SM (2016) Both estrogen and androgen modify the response to activation of neurokinin-3 and κ-opioid receptors in arcuate kisspeptin neurons from male mice. Endocrinology 157:752–763.

Schauberger P, Walker A (2020) openxlsx: read, write and edit xlsx files (R package version 4.2.3). Available at https://cran.r-project.org/package=openxlsx.

Schloerke B, Cook D, Larmarange J, Briatte F, Marbach M, Thoen E, Elberg A, Crowley J (2020) GGally: extension to "ggplot2" (R package version 2.0.0). Available at https://cran.r-project.org/package=GGally.

Silva MSB, Desroziers E, Hessler S, Prescott M, Coyle C, Herbison AE, Campbell RE (2019) Activation of arcuate nucleus GABA neurons promotes luteinizing hormone secretion and reproductive dysfunction: implications for polycystic ovary syndrome. EBioMedicine 44:582–596.

Simonoff JS (2003) Multidimensional contingency tables. In: Analyzing categorical data. Springer texts in statistics, pp 309–364. New York: Springer.

Smith JT, Dungan HM, Stoll EA, Gottsch ML, Braun RE, Eacker SM, Clifton DK, Steiner RA (2005) Differential regulation of KiSS-1 mRNA expression by sex steroids in the brain of the male mouse. Endocrinology 146:2976–2984.

Sullivan SD, Moenter SM (2004) Prenatal androgens alter GABAergic drive to gonadotropin-releasing hormone neurons: implications for a common fertility disorder. Proc Natl Acad Sci USA 101:7129–7134.

Sullivan SD, Moenter SM (2005) GABAergic integration of progesterone and androgen feedback to gonadotropin-releasing hormone neurons. Biol Reprod 72:33–41.

Underwood AJ (1997) Experiments in ecology: their logical design and interpretation using analysis of variance. Cambridge: Cambridge University Press.

Vanacker C, Moya MR, DeFazio RA, Johnson ML, Moenter SM (2017) Long-term recordings of arcuate nucleus kisspeptin neurons reveal patterned activity that is modulated by gonadal steroids in male mice. Endocrinology 158:3553–3564.

Veiga-Lopez A, Ye W, Phillips DJ, Herkimer C, Knight PG, Padmanabhan V (2008) Developmental programming: deficits in reproductive hormone dynamics and ovulatory outcomes in prenatal, testosterone-treated sheep. Biol Reprod 78:636–647.

Walters KA, Edwards MC, Tesic D, Caldwell ASL, Jimenez M, Smith JT, Handelsman DJ (2018) The role of central androgen receptor actions in regulating the hypothalamic-pituitary-ovarian axis. Neuroendocrinology 106:389–400.

Wickham H, Hester J (2020) readr: read rectangular text data (R package version 1.4.0). Available at https://cran.r-project.org/package=readr.

Wickham H, Seidel D (2020) scales: scale functions for visualization (R package version 1.1.1). Available at https://cran.r-project.org/package=scales.

Wickham H, Averick M, Bryan J, Chang W, McGowan L, François R, Grolemund G, Hayes A, Henry L, Hester J, Kuhn M, Pedersen T, Miller E, Bache S, Müller K, Ooms J, Robinson D, Seidel D, Spinu V, Takahashi K, et al. (2019) Welcome to the Tidyverse. J Open Source Softw 4:1686.

Wickham H, François R, Henry L, Müller K (2020) dplyr: a grammar of data manipulation (R package version 1.0.2). Available at https://cran.r-project.org/package=dplyr.

Wildt L, Häusler A, Marshall G, Hutchison JS, Plant TM, Belchetz PE, Knobil E (1981) Frequency and amplitude of gonadotropin-releasing hormone stimulation and gonadotropin secretion in the rhesus monkey. Endocrinology 109:376–385.

Wilke CO (2020) cowplot: streamlined plot theme and plot annotations for "ggplot2" (R package version 1.1.1.). Available at https://cran.r-project.org/package=cowplot.

Xie Y (2014) knitr: a comprehensive tool for reproducible research in R. In: Implementing reproducible research (Stodden V, Leisch F, Peng RD, eds). Boca Raton: Chapman and Hall/CRC.

Xie Y (2015) Dynamic documents with R and knitr, Ed 2. Boca Raton: Chapman and Hall/CRC.

Xie Y (2020) knitr: a general-purpose package for dynamic report generation in R. Available at https://yihui.org/knitr/.

Xie Y, Cheng J, Tan X (2021) DT: a wrapper of the JavaScript library "DataTables" (R package version 0.18). Available at https://cran.r-project.org/package=DT.

Yan X, Yuan C, Zhao N, Cui Y, Liu J (2014) Prenatal androgen excess enhances stimulation of the GNRH pulse in pubertal female rats. J Endocrinol 222:73–85.

Yip SH, Boehm U, Herbison AE, Campbell RE (2015) Conditional viral tract tracing delineates the projections of the distinct kisspeptin neuron populations to gonadotropin-releasing hormone (GnRH) neurons in the mouse. Endocrinology 156:2582–2594.

Zhu H (2020) kableExtra: construct complex table with "kable" and pipe syntax (R package version 1.3.1). Available at https://cran.r-project.org/package=kableExtra.